JOURNAL OF GEOPHYSICAL RESEARCH, VOL. 100, NO. C5, PAGES 8639–8653, MAY 15, 1995

Synoptic bottom pressure variability on the Labrador and Newfoundland Continental Shelves

Brad deYoung, Youyu Lu, and Richard Greatbatch
Department of Physics, Memorial University of Newfoundland, St. John's, Canada

Abstract. A high-resolution, barotropic model of the North Atlantic is used to investigate bottom pressure variability on the Labrador and Newfoundland Shelves. The model has a free surface and is forced by surface atmospheric pressure and wind stress derived from twice-daily analyses from the European Centre for Medium-Range Weather Forecasts. Model output is compared with a yearlong set of bottom pressure data (1985-1986). Coherence squared between model and observations is significant at the 95% confidence level at almost all stations and exceeds 0.6 over most of the inner shelf, with good agreement in the phase. The model shows a tendency to overestimate the autospectral energy at periods less than 10 days but to underestimate the energy at longer periods. The model does less well at the outer shelf, where coherence squared is only marginally significant. The weaker performance of the model near the shelf break may indicate a role for physical processes not accounted for in the model (e.g., eddies, stratification) or, alternatively, might be due to the low signal-to-noise ratio in the bottom pressure measurements made at the shelf break. Model/data comparisons show that wind forcing dominates over pressure forcing, except at the northern end of the Labrador Shelf, where both forcings are important. Model experiments run with and without Hudson Bay in the model domain demonstrate that Hudson Bay influences the Labradr Shelf in the 2 to 10-day period range.

1. Introduction

In this paper we use a high-resolution model of the North Atlantic Ocean to study bottom pressure measurements made on the Newfoundland and Labrador Shelves. These shelves provide an interesting area in which to study bottom pressure variability because of the presence of a broad (but rugged) continental shelf, strong wind forcing, and the potential influence of neighboring seas. Figure 1a shows the study area, together with the location of the bottom pressure measurements. These were made in the area from 1985 to 1987 [*Wright et al.*, 1988].

Previous studies of the Newfoundland and Labrador Shelves have applied both empirical and numerical analysis. At the seasonal timescale, *Thompson et al.* [1986] used multiple-regression analysis applied to Nain sea level data to extract both the local wind-driven signal and the influence of wind forcing over the North Atlantic. *Greatbatch et al.* [1990] (hereinafter referred to as GDGC) confirmed Thompson et al.'s analysis using a barotropic numerical model driven by the seasonally varying wind stress field of *Hellerman and Rosenstein* [1983]. GDGC were able to separate the local wind set up from the influence of wind forcing over the North Atlantic by embedding a model of the shelf in a coarse resolution model of the North Atlantic [*Greatbatch and Goulding,* 1989]. A significant portion of the seasonal sea level signal on the Labrador Shelf was found to be influenced by the North Atlantic. GDGC were also able to separate the seasonal sea level signal at St. John's, Newfoundland, into parts associated with wind forcing and the seasonal steric effect.

Unanswered questions remain at the synoptic timescales. An empirical analysis applied by *Garrett et al.* [1985] suggested that the response of sea level at Nain, Labrador, to atmospheric pressure is significantly nonisostatic at ~2 to 10-day period. This deviation was not expected [*Wunsch,* 1972; *Ponte et al.,* 1991] and it motivated *Wright et al.* [1987] to conclude that the nonisostatic response was because of a resonant response of Hudson Bay and Hudson Strait to atmospheric pressure forcing. *Wright et al.* [1987] applied a simple dynamical model to demonstrate the effect, suggesting that it could be important for periods of 2-6 days. They concluded that this explained the discrepancy found by *Garrett et al.* [1985] but claimed that the variation of wind, as distinct from atmospheric pressure, over Hudson Bay was not important. *Webster and Narayanan* [1988] applied a barotropic model with a rigid lid, in an effort to explain observed current variability on the northern Labrador Shelf. They identified the influence

Paper number 95JC00231
0148-0227/95/95JC-00231$05.00

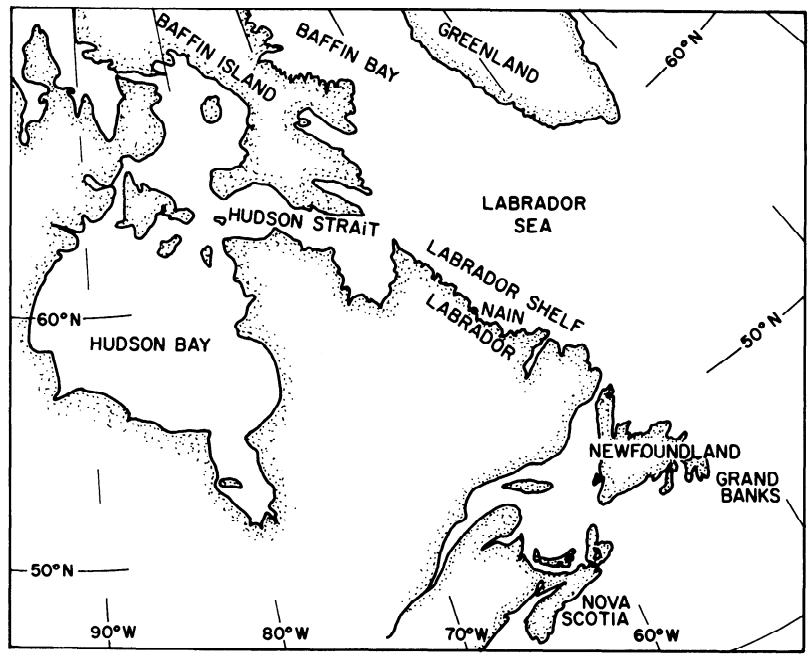

Figure 1a. Bottom topography of the northwest Atlantic showing Hudson Bay, the Labrador Sea and Shelf, and the Grand Banks of Newfoundland.

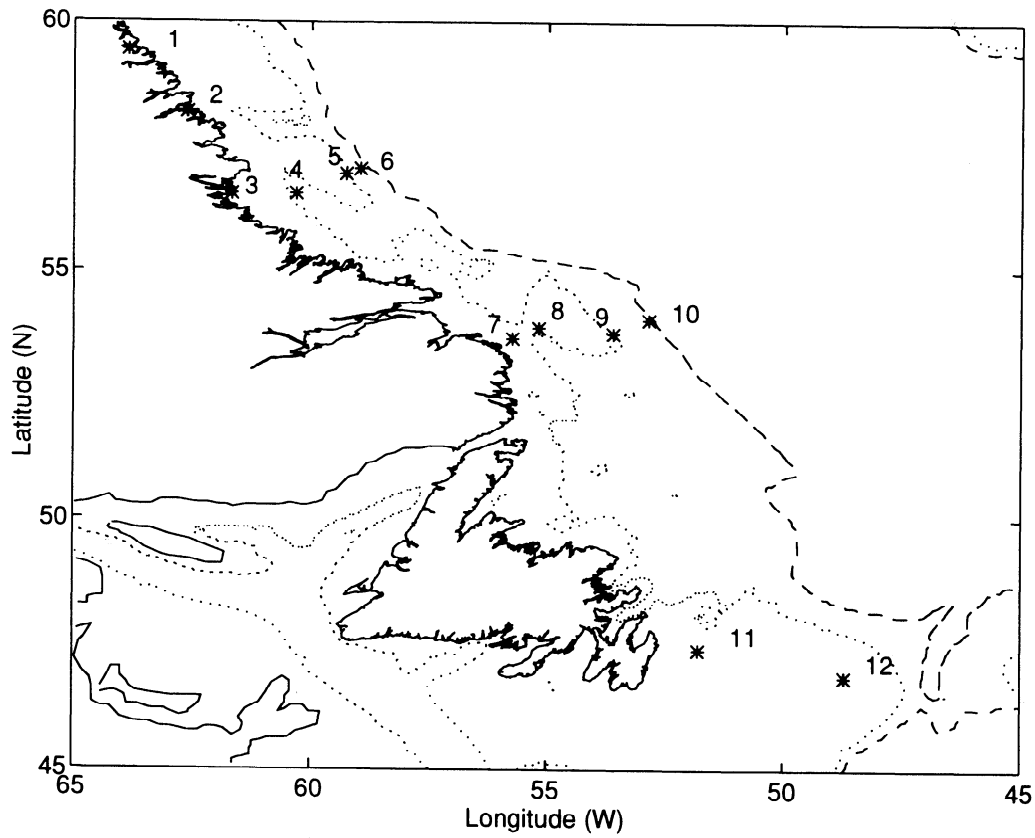

Figure 1b. Location of the station data showing (1) Hebron, (2) Brownell, (3)-(6) Nain stations, (7)-(10) Hamilton Bank stations, and (11) and (12) the Grand Banks stations. The data set roughly covers the period June 1985 to August 1987. See Table 1 for a complete listing of the station names, positions, start times, and record lengths. Only the 200- and 500-m bottom contours are shown.

of Hudson Bay and Hudson Strait, at 2.8 to 5.5-day periods. Their model was not successful at periods of 1.8-2.8 days and 5.5-11 days. They suggested that the influence of wind forcing in regions not considered in the model, e.g., Hudson Bay and Baffin Bay, might be needed to explain this discrepancy.

An array of bottom pressure gauges, with record lengths of 292 to 390 days, was deployed on the Labrador Shelf from June 1985 to July 1987, as described by *Wright et al.* [1988]. These gauges ran across and along the shelf (Figure 1) and provide a fairly complete set of data for exploring the nonisostatic response to wind and atmospheric pressure forcing. *Middleton and Wright* [1989] applied a dynamical mode fitting technique to explain the observed bottom pressure variability in terms of coastal trapped waves (CTWs). In a later study, *Middleton and Wright* [1991] included the effect of local wind forcing and offshore influence which they describe as a "Kelvin wave" mode (such as described by *Davis and Bogden* [1989]). The influence of scattering by the topography was added by *Wright et al.* [1991], who used multiple regression analysis to show that the amplitude of the CTWs decreases more rapidly along the real shelf than it would on a smooth shelf. The influence of the offshore in their model was included via a pressure term at the shelf break. *DeYoung et al.* [1992] (hereinafter referred to as DGGV) applied a model like that of GDGC, except that it was forced using European Centre for Medium-Range Weather Forecasts (ECMWF) twice-daily winds. The model was run in the frequency domain and used to investigate three discrete time periods, 4, 8, and 12 days. The influence of remote forcing from the North Atlantic was incorporated by running the coarse resolution model of *Greatbatch and Goulding* [1989] with twice-daily forcing. Strong coherence between the model and data was found at the 4- and 8-day periods near the coast, but the model underestimated the amplitude of the response. They were not able to determine the influence of Hudson Bay because of difficulty incorporating the Hudson Strait boundary condition in the model.

The successful, although somewhat mixed, results of the various modeling attempts provided encouragement for us to carry on this work with some clear questions in mind. Can a barotropic model account for the observed variance at synoptic periods on the shelf, or is it necessary to include stratification? What is the influence of Hudson Bay on the Labrador Shelf, and at what periods does it play a role? What is the relative importance of pressure and wind stress forcing on the shelves? We shall address these questions in this paper. In the next section we shall describe the barotropic model used in our study, followed by a discussion of the model results, together with some discussion of the data. In the final section we shall provide a summary and suggest some conclusions that can be drawn.

2. Model

In our previous studies of bottom pressure and sea level variability on the shelf we applied a barotropic stream function model that had a rigid lid and was solved in the frequency domain [*Greatbatch and Goulding*, 1989; *Greatbatch et al.*, 1990; *deYoung et al.*, [1992]. While successful, particularly in elucidating the seasonal signal, we now relax the rigid-lid condition and work in the time domain. This allows us to include atmospheric pressure forcing and enables us to make a more complete comparison between model output and observations. The model that we shall apply is barotropic and linear, except for the bottom friction term.

DeYoung et al. [1992] found that including the effect of density stratification in their model did not lead to any significant change in their results. This is because the ratio of the baroclinic Rossby radius of deformation

Table 1. Locations, Depths, and Time Information for the Bottom Pressure Data

Number	Station	Depth, m	Latitude, °N	Longitude, °W	Start Date	Length, days
1	Brownell	<5	59.42	63.85	Aug. 12, 1985	357
2	Hebron	<5	58.18	62.62	Aug. 12, 1985	357
3	Nain1	<5	56.55	61.68	Aug. 11, 1985	357
4	Nain2	204	56.55	60.32	Oct. 18, 1985	292
5	Nain3	175	56.95	59.26	Oct. 17, 1985	292
6	Nain4	571	57.05	58.96	Oct. 17, 1985	292
7	Hamilton1	109	53.63	55.74	July 7, 1985	390
8	Hamilton2	145	53.84	55.18	July 7, 1985	390
9	Hamilton3	200	53.73	53.61	June 7, 1985	390
10	Hamilton4	600	54.01	52.85	June 7, 1985	390
11	Grand1	183	47.40	51.80	April 23, 1985	372
12	Grand2	98	46.86	48.72	April 24, 1985	372

Locations of the instruments are shown in Figure 1b. In the text the locations are referred to by their station name.

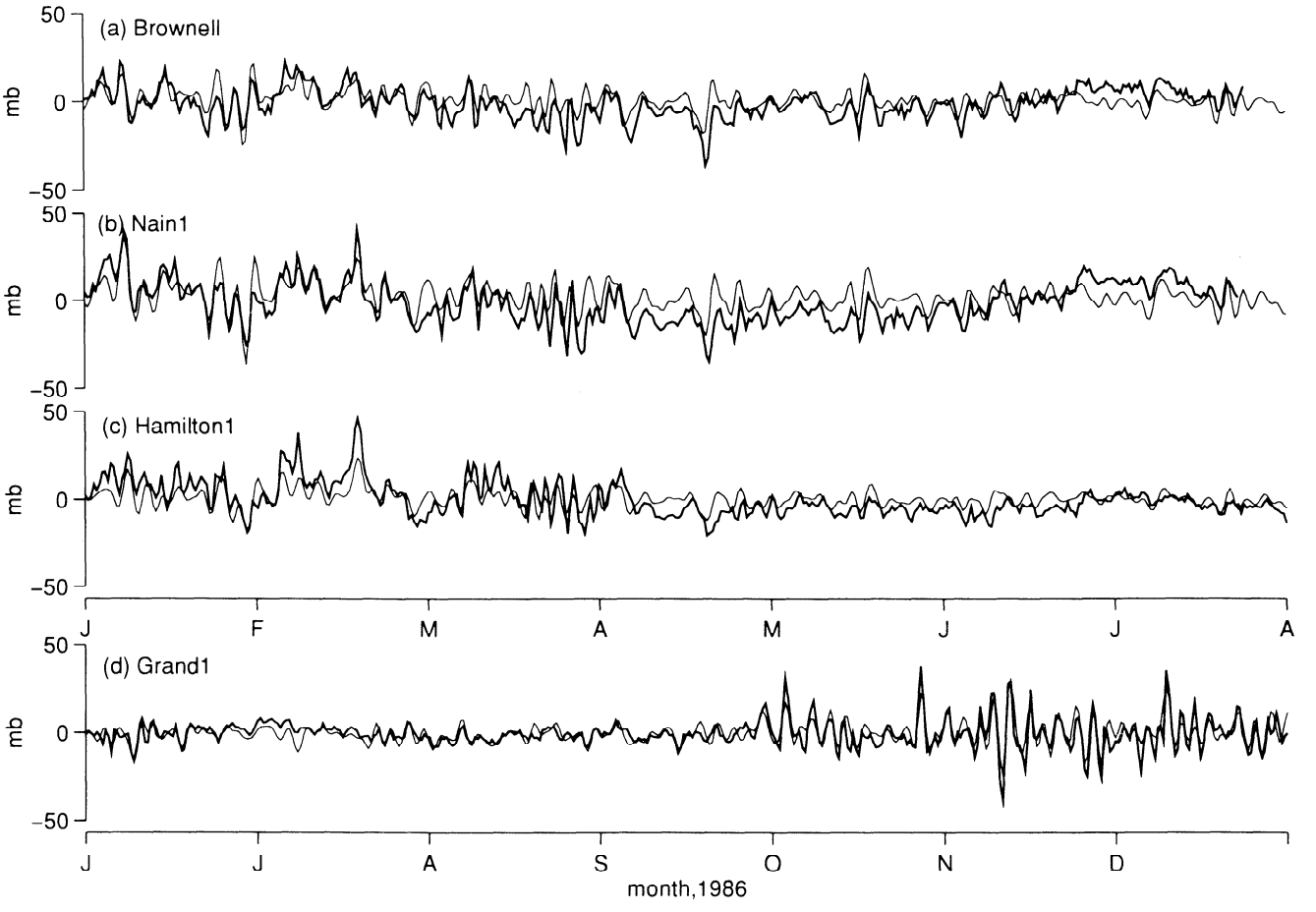

Figure 2. Time series of bottom pressure at (a) Brownell (1), (b) Nain1 (3), (c) Hamilton1 (7), and (d) Grand1 (11), with numbers in parentheses corresponding to the numbers used to identify the stations in Table 1 and Figure 1b. Note that the pressure is plotted in millibars, where 1 mb $\cong$ 1 cm of adjusted sea level. Also note that the Grand Banks data start at the month of July, while the three northern stations start in January. Both observed data (thick line) and the results of the wind and pressure forced model (thin line) are plotted.

to the shelf width is of order 0.02 for the Labrador and Newfoundland Shelves [*Middleton and Wright,* 1990]. We therefore neglect baroclinic effects and base our model on the vertically integrated shallow water equations for a homogeneous ocean [*Gill,* 1982]. Including wind and atmospheric pressure forcing, the governing equations in spherical coordinates are

$$\frac{\partial \eta}{\partial t} + \frac{1}{a\cos\phi}\left[\frac{\partial}{\partial \lambda}(Hu) + \frac{\partial}{\partial \phi}(Hv\cos\phi)\right] = 0 \quad (1)$$

$$\frac{\partial u}{\partial t} - 2\Omega \sin\phi\, v = -\frac{g}{a\cos\phi}\frac{\partial}{\partial \lambda}\left(\eta + \frac{p_a}{\rho_o g}\right) + \frac{\tau_s^\lambda - \tau_b^\lambda}{\rho_o H} + A_h f^\lambda \quad (2)$$

$$\frac{\partial v}{\partial t} + 2\Omega \sin\phi\, u = -\frac{g}{a}\frac{\partial}{\partial \phi}\left(\eta + \frac{p_a}{\rho_o g}\right) + \frac{\tau_s^\phi - \tau_b^\phi}{\rho_o H} + A_h f^\phi \quad (3)$$

where η is the upward displacement of sea level, a is the radius of the Earth, ϕ is the latitude, λ is the longitude, H is the water depth, u and v are the eastward and northward components of velocity, respectively, Ω is the rotation rate of the Earth, g is the acceleration due to gravity, A_h is the horizontal eddy viscosity, p_a is the atmospheric pressure, and ρ_o is a representative density for seawater (here 1025 kg m^{-3}). The τ_s^λ and τ_s^ϕ are the eastward and northward components of the surface wind stress. τ_b^λ and τ_b^ϕ are the components of bottom stress which are related to the velocity field by a quadratic bottom friction law

$$(\tau_b^\lambda, \tau_b^\phi)/\rho_o = k(u^2 + v^2)^{1/2}(u, v)$$

where k is the empirical quadratic bottom friction coefficient. Lateral mixing is parameterized following *Bryan* [1969]

$$f^\lambda = \frac{1}{a^2\cos^2\phi}\frac{\partial^2 u}{\partial \lambda^2} + \frac{1}{a^2\cos\phi}\frac{\partial}{\partial \phi}\left(\cos\phi\frac{\partial u}{\partial \phi}\right) + \frac{1}{a^2}\left[(1 - \tan^2\phi)u - \frac{2\tan\phi}{\cos\phi}\frac{\partial v}{\partial \lambda}\right] \quad (4)$$

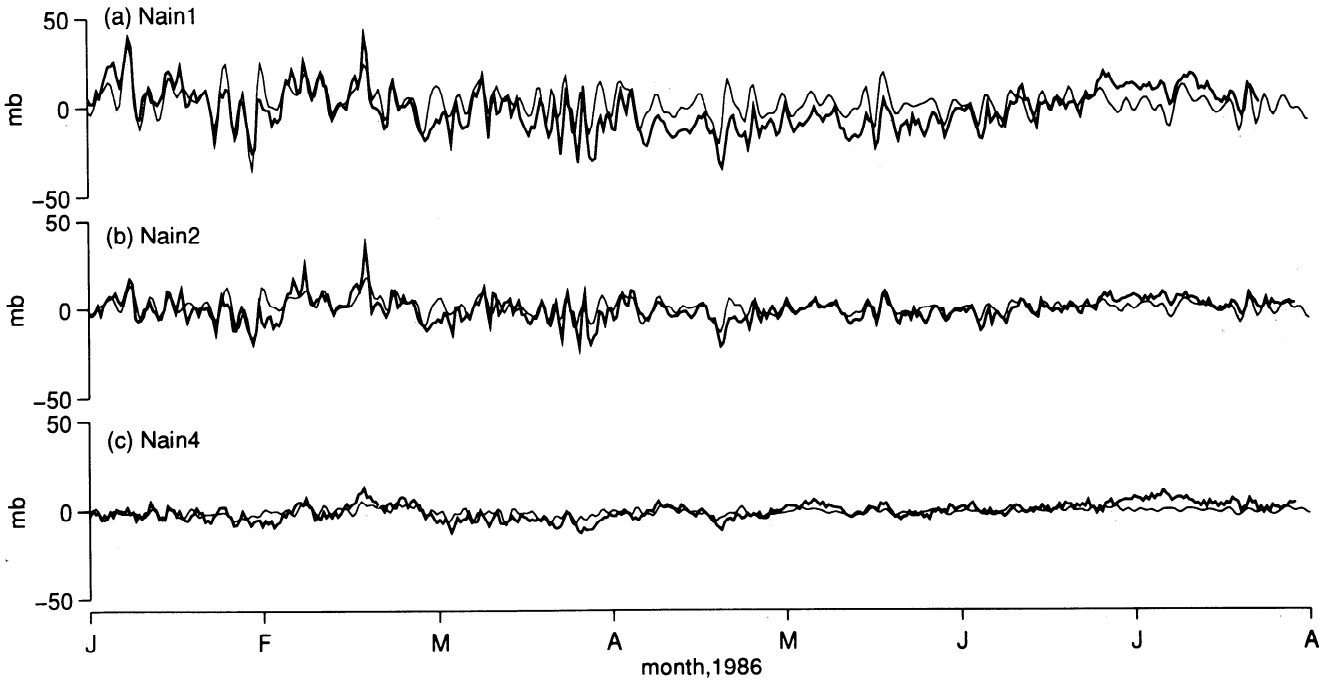

Figure 3. Time series of bottom pressures at (a) Nain1 (3), (b) Nain2 (4), and (c) Nain4 (6), with numbers in parentheses corresponding to the numbers used to identify the stations in Table 1 and Figure 1b. The pressure is plotted as millibars, where 1 mb $\cong$ 1 cm of adjusted sea level. Both data (thick line) and the results of the wind and pressure forced model (thin line) are plotted.

$$f^{\phi} = \frac{1}{a^2\cos^2\phi}\frac{\partial^2 v}{\partial\lambda^2} + \frac{1}{a^2\cos\phi}\frac{\partial}{\partial\phi}(\cos\phi\frac{\partial v}{\partial\phi}) + \frac{1}{a^2}[(1-\tan^2\phi)v + \frac{2\tan\phi}{\cos\phi}\frac{\partial u}{\partial\lambda}] \quad (5)$$

To solve these equations, we use the finite difference method described by *Heaps* [1971]. The spatial differential operators are calculated using centered differencing on the C grid. Forward time differencing is applied to (1) and backward differencing to (2) and (3), except for the Coriolis term in (2) which is calculated using forward time differencing. The lateral and bottom friction terms are treated explicitly.

The bottom topography adopted in our model experiments is the same as that used by *Bryan and Holland* [1989] in their eddy-resolving general circulation model of the North Atlantic, except that we close the model domain at the equator and the Hudson Bay–Hudson Strait system is included (Figure 1). The resolution is 1/3° in latitude and 2/5° in longitude, giving an equal grid spacing in the north-south and east-west directions of about 37 km at 34°N. The topography is stepwise (with 30 discrete depth levels) and designed for three-dimensional, level models. The topography of Hudson Bay–Hudson Strait was first extracted from a digital terrain data set (with a resolution of 1/12° × 1/12°), then linearly interpolated to the 1/3° × 2/5° grid and discretized to the closest discrete level, and finally merged with the North Atlantic topography. In some of the model experiments the Hudson Bay–Hudson Strait system is closed in order to determine its influence on the Labrador and Newfoundland shelves. A "no-slip" boundary condition is applied along the coastal boundaries and also along the northern and southern boundaries of the model domain (i.e., at the equator and 65°N). The surface pressure and wind fields used to drive the model are twice-daily analyses from the ECMWF for the years 1985 and 1986. The wind and atmospheric pressure fields are interpolated to the model grid using the interpolation scheme of *Akima* [1978]. The wind stress is then calculated using the formula of *Large and Pond* [1981], and the forcing fields are linearly interpolated in time to the model time step.

In the model runs to be described the quadratic bottom friction and horizontal eddy viscosity coefficients have values $k = 2.5 \times 10^{-3}$ and $A_h = 10^3$ m^2 s^{-1}, respectively. These values of k and A_h reproduce the correct pattern of amphidromic points under tidal forcing, suggesting their appropriateness for our study. Sensitivity tests showed that the model results are not strongly dependent upon the value of A_h. The model is initialized with $u = v = \eta = 0$ at 0000 UT on January 1, 1985. After about 3 weeks integration the model has forgotten its initial condition.

3. Model Results

The data set we explore was obtained by *Wright et al.* [1988, 1991] and is one that has already be analyzed

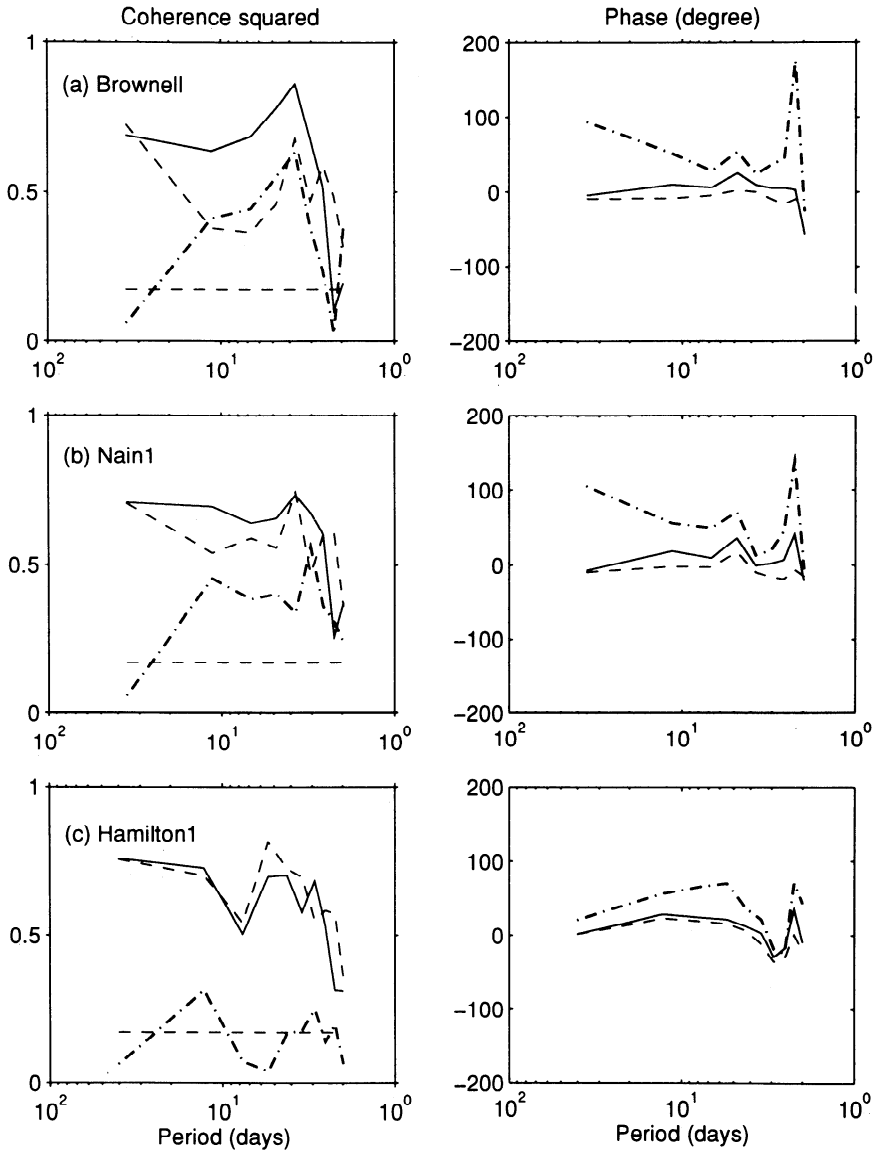

Figure 4. Coherence squared and phase between the model output and the data at (a) Brownell, (b) Nain1, and (c) Hamilton1. The 95% confidence limit for the coherence squared is shown as a horizontal dashed line. Results are shown for the wind and pressure forced model (solid line), the wind only forced model (dashed line), and pressure only forced (dot-dashed line). Positive phase means that the observed data lead the model.

by different groups (see Introduction). The time series of bottom pressure are from 292 to 390 days in length, extending over the period from the summer of 1985 to the summer of 1987 (see Table 1). The northern gauges were deployed in 1985 (stations 1-10 in Figure 1b) and the southern gauges in 1986 (stations 11-12 in Figure 1b). Tidal constituents in the data have been removed by harmonic analysis and a low-pass filter applied. The filter passed all energy at periods greater than 2 days, leaving less than 2% of the energy at periods less than 1 day. A similar low-pass filter was applied to the model output. For this reason, we do not consider periods less than 2 days in the following analysis.

We shall present results from the following three different model experiments: (1) those forced by both wind and pressure, (2) those forced by pressure only, and (3) those forced by wind only. Figures 2 and 3 compare time series of observed bottom pressure with model results from case 1 (that is, forced by both wind and pressure). Figure 2 shows time series for near-shore stations from Brownell in the north to Grand1 in the south (see Figure 1), whereas Figure 3 shows time series at stations extending from the coast to the shelf break at Nain, a distance of about 150 km.

Looking first at the observed time series, we can see from Figure 2 that there are coherent structures along

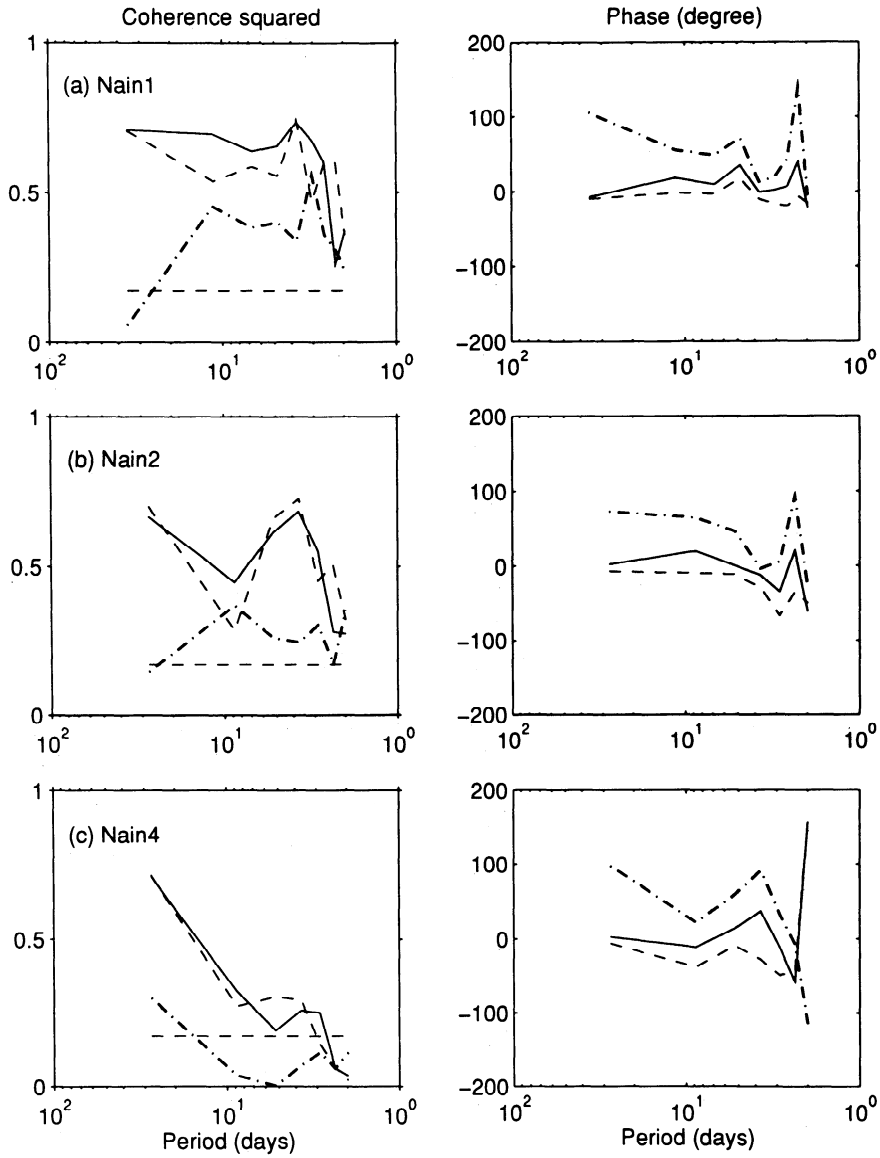

Figure 5. Coherence squared and phase between the model output and the data at (a) Nain1, (b) Nain2, and (c) Nain4. The 95% confidence limit for the coherence squared is shown as a horizontal dashed line. Results are shown for the wind- and pressure-forced model (solid line), the wind only forced model (dashed line), and pressure only forced model (dot-dashed line). Positive phase means that the observed data lead the model.

the shelf at different periods, although clear differences can also be seen between Brownell and Hamilton, where the station separation is roughly 1100 km. Between the Labrador Shelf and the Grand Banks there is some coherence, but it is weak [*Wright et al.*, 1991]. Across the shelf (Figure 3), from near the shore to the shelf break (see Figure 1b), there is also strong coherence. There is also a decrease in amplitude across the shelf, indicating that energy is coastally trapped.

Comparing model and observations in Figures 2 and 3, we see that, in general, the model does well at synoptic periods, however, at longer periods there are discrepancies. An example occurs in spring at Nain1 (Figure 2), a discrepancy that may be associated with baroclinic effects (for example, long-period fluctuations in the offshore Labrador Current). The model does extremely well on the Grand Banks (coherence squared between model and observations is above 0.7). This agreement is probably because the bank has closed isobaths running around it. Looking at Figure 3, we see that both the observed and model-computed time series show a decrease in amplitude as one moves offshore. This decrease in amplitude makes visual comparison of the two time series difficult at the offshore stations. A better approach is to calculate coherence squared and phase (Figure 4). For the case with both wind and pressure forcing (Fig-

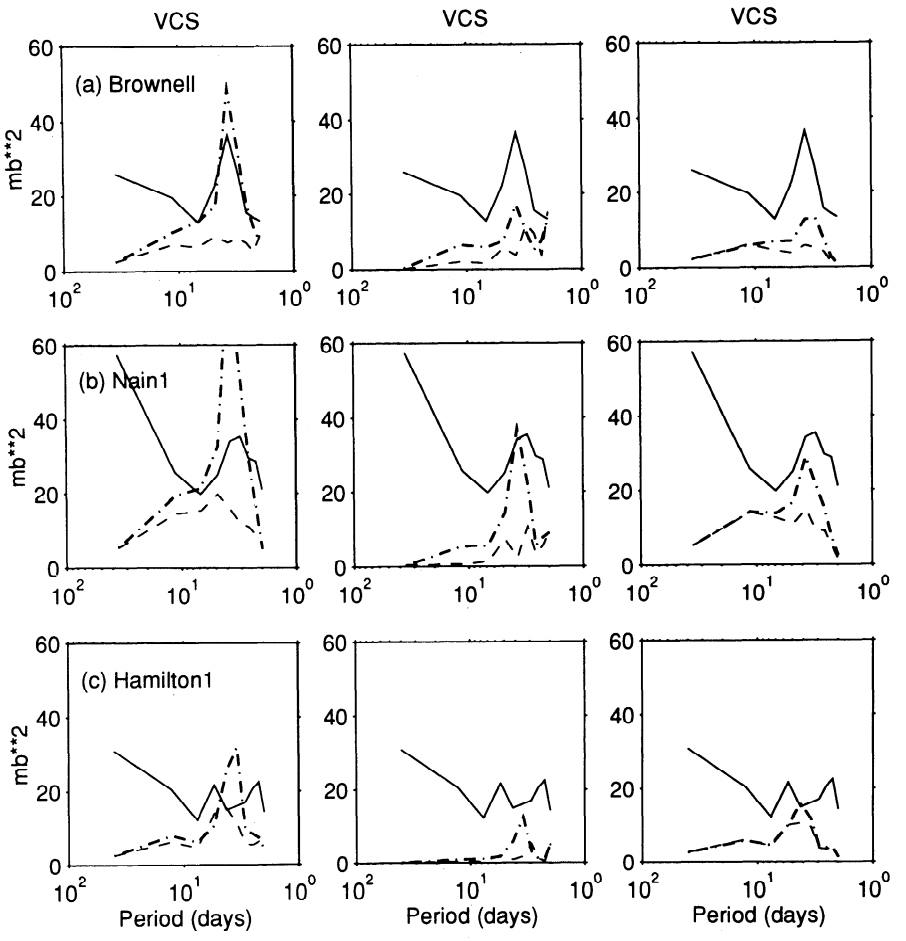

Figure 6. Autospectra for the observed data (solid line) in variance-preserving form at (a) Brownell, (b) Nain1, and (c) Hamilton1. Model results are for the Hudson Bay open (dot-dashed line) and closed (dashed line) casess are also shown. The left column shows the results for the model run with wind and pressure forcing, the middle column for the case forced by pressure only, and the right column for the case forced by wind only.

ure 4, solid line) the coherence squared ranges from 0.5 to 0.8 along the shelf, significant at all periods from 2-40 days. Although there is strong coherence over the inner shelf, Figure 5 shows that the coherence squared drops off at the outer stations, particularly at periods less than 10-20 days. The phase plots in Figure 4 show that where the coherence is high, the model is almost in phase with the data, a result confirmed by looking at Figures 2 and 3. Despite the high coherence at all stations at long periods, the model underestimates the energy at periods greater than 10 days, as can be seen in Figure 6 for the case of the inshore stations. We have already noted that discrepancies between model and data can be seen at longer periods in Figures 2 and 3.

We can also use the model to investigate the relative importance of the wind and atmospheric pressure forcing. The case with atmospheric pressure forcing alone (the dot-dashed line in Figures 4 and 5) shows significant coherence with the observations from Nain northward but generates almost no significant coherence at Hamilton. At the far northern stations, Brownell and Hebron (not shown), the model performs better when forced with both wind and atmospheric pressure than when forced by wind alone. These results indicate the importance of pressure forcing on the northern part of the shelf. It is interesting to note that the phase of the wind only model matches the data well (even at Brownell) but that the pressure only model run shows a consistent phase difference with the data, lagging the data by up to 100° and showing that both forcings are necessary to obtain agreement with observations.

Spectra for the data and the model show that pressure forcing (Figure 6) is roughly equal in importance to wind forcing at the northern end of the shelf but becomes less important farther south at Hamilton Bank, where wind forcing dominates. Still farther south, on the Grand Banks, atmospheric pressure forcing plays

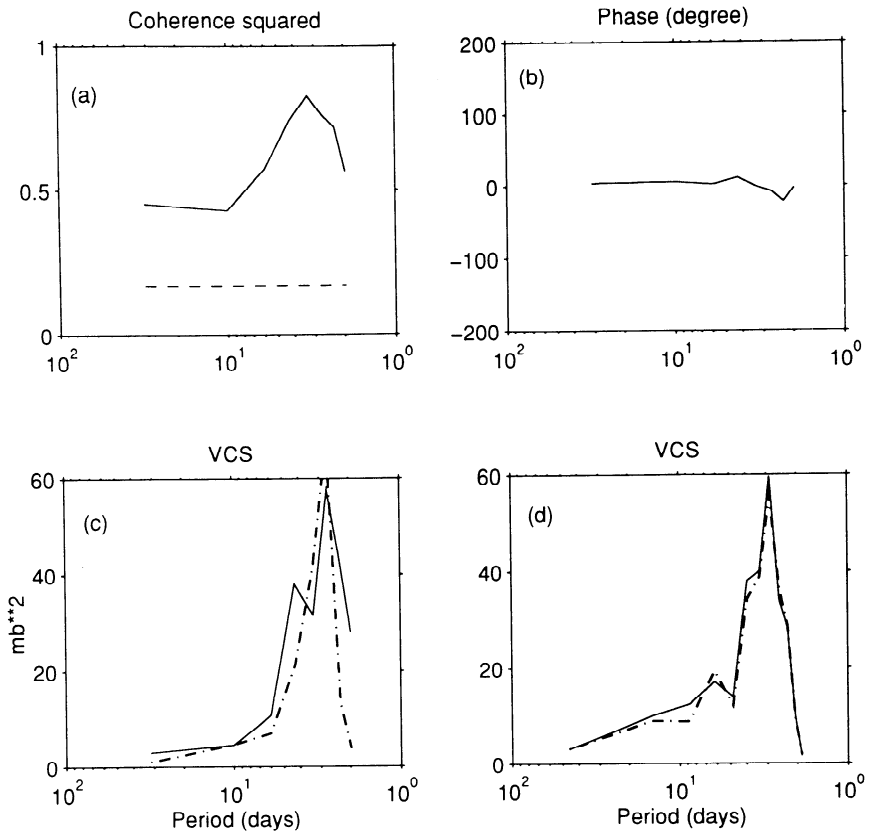

Figure 7. (a) Coherence squared and (b) phase between the observed data and the model run with both wind and pressure forcing at Grand1 on the Grand Banks. The 95% confidence limit for the coherence squared is shown as a horizontal dashed line. Positive phase means that the observations lead the model. Variance-preserving autospectra for the data (solid line) and for the model results with Hudson Bay (c) open and (d) closed are also shown (dot-dashed line). There are slight differences between the dot-dashed line in Figure 7c and the solid line in Figure 7d because they are calculated for different periods in 1986.

only a minor role. We commented earlier that on the Grand Banks the model does particularly well. Figure 7 shows that the coherence squared at Grand1 rises from 0.5 at long periods to roughly 0.8 at about 6 days. The model also does a good job at simulating the variance on the banks.

The influence of Hudson Bay and Hudson Strait was first raised by *Wright et al.* [1987] as providing an explanation for the results of an earlier study of observed sea level study at Nain [*Garrett et al.*, 1985]. In a previous modeling effort (DGGV) we attempted to account for the influence of Hudson Bay and Hudson Strait by imposing a forcing function in the model at the location of the mouth of Hudson Strait, as done by *Webster and Narayanan* [1988]. Our earlier effort did not succeed, and so in this study we explicitly include Hudson Bay in the model domain. To test the influence of the bay and strait, we repeated our model runs, but with Hudson Strait closed off. Plots of coherence squared along the shelf show a dramatic decrease in coherence at the northern stations if Hudson Bay is absent (see Figure 8). The effect is reduced farther south and is almost entirely absent at Hamilton Bank (Figure 8). The phase is not sensitive to the presence or absence of Hudson Bay. Farther to the south, on the Grand Banks, there is no discernible influence of Hudson Bay, with coherence squared barely changing and almost no difference between the autospectra for the case when Hudson Bay is open (solid line in Figure 7c) or closed (dot-dashed line in Figure 7d).

The contribution of Hudson Bay to the model-computed variance is also apparent from a comparison of the dot-dashed and dashed lines in Figure 6. Indeed, including Hudson Bay is necessary if the model is to reproduce the energy peak near 4 days at Brownell and Nain1, although the model clearly overestimates this peak. It may be that the topography in our model is too smooth and does not adequately scatter waves incident upon the northern end of the Labrador Shelf. Too much energy may exit Hudson Strait and be transferred to the Labrador Shelf. More realistic topography, using even higher resolution, may be needed to account prop-

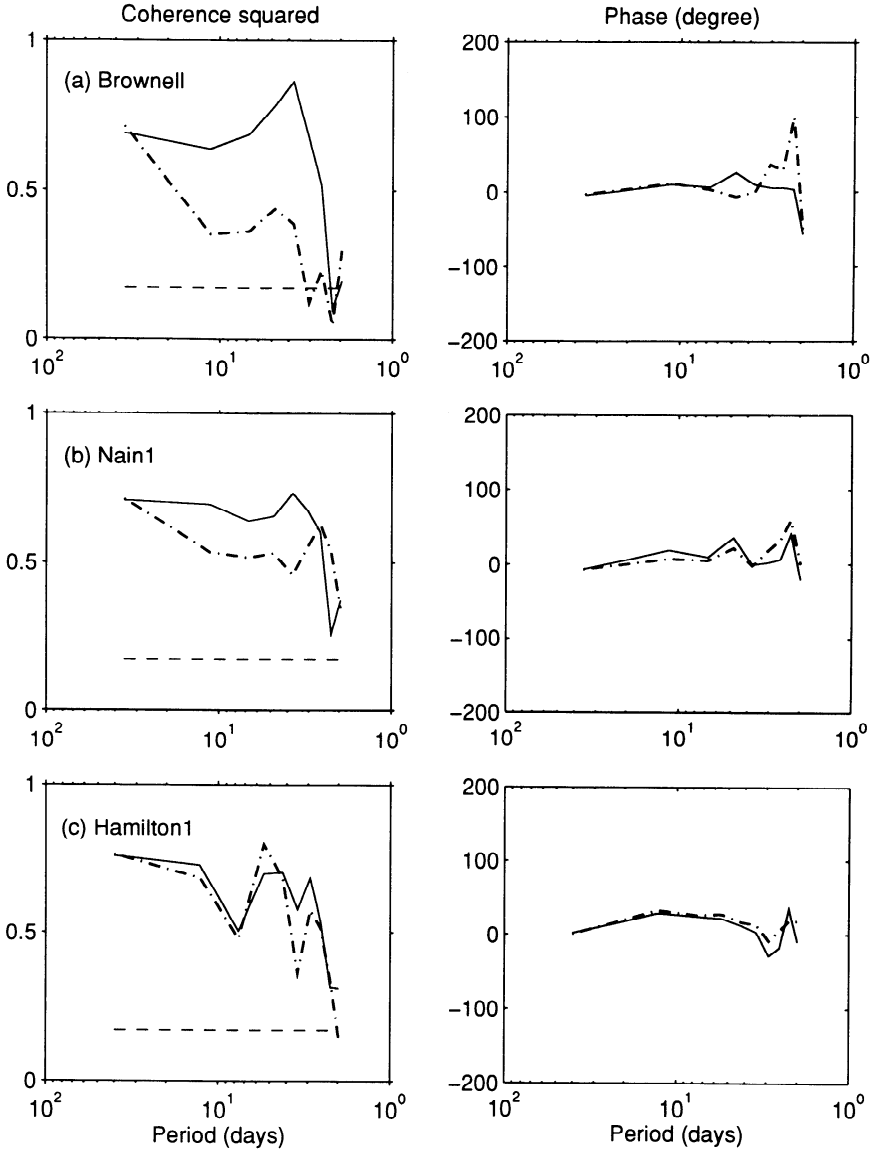

Figure 8. Coherence squared and phase between observed data and wind- and pressure-forced model runs with Hudson Bay open (solid line) and closed (dot-dashed line) at (a) Brownell, (b) Nain1, and (c) Hamilton1. The 95% confidence limit for the coherence squared is shown as a horizontal dashed line.

erly for the transfer of energy onto the Labrador Shelf. It may also be that this discrepancy arises because of local measurement problems or problems associated with interpolating the model output to the observation location (i.e., a higher resolution model may be needed to account for local topographic features near the measurement location that might be playing a role).

We have tested the frequency dependence of the model response to Hudson Bay by driving the model using an idealized atmospheric pressure forcing and no wind forcing. We forced the model with a zonally uniform atmospheric pressure field, the latitudinal structure of which is shown in Figure 9. The pressure between the equator and 40°N is oscillated up and down using a white noise spectrum in the frequency domain. There is no horizontal pressure gradient in the northern part of the domain (Figure 9b), and, in particular, there is no abrupt gradient in pressure near the mouth of Hudson Bay. In Figure 10 we plot the ratio of the model-computed sea level to the inverse barometer for cases with Hudson Bay open (the solid line in Figure 10) or closed (dashed line in Figure 10). When Hudson Bay is closed, the ratio of amplitudes is flat from long periods down to 2 days, where the inverse barometer approximation breaks down [*Ponte et al.*, 1991]. With Hudson Bay open there is a clear discrepancy at periods of 4-10 days, thus confirming the resonator model of *Wright et al.* [1987] and providing a clear indication of the fre-

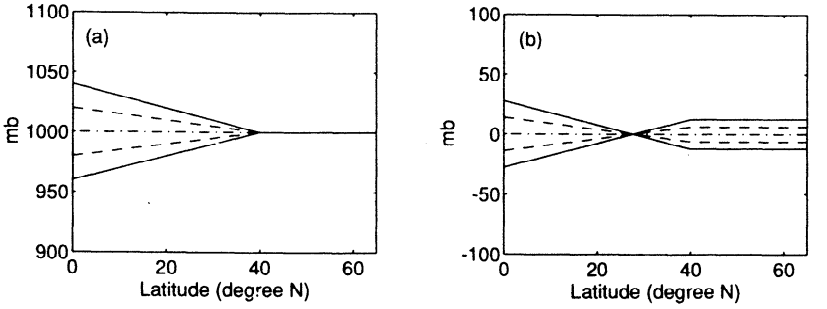

Figure 9. (a) The north-south structure of the zonally uniform atmospheric pressure field used to force the idealized model, $p_a = 1000 + A(\phi)\alpha(t)$ (see the text). (b) The north-south structure of the pressure difference field $(p_a - p_b)$.

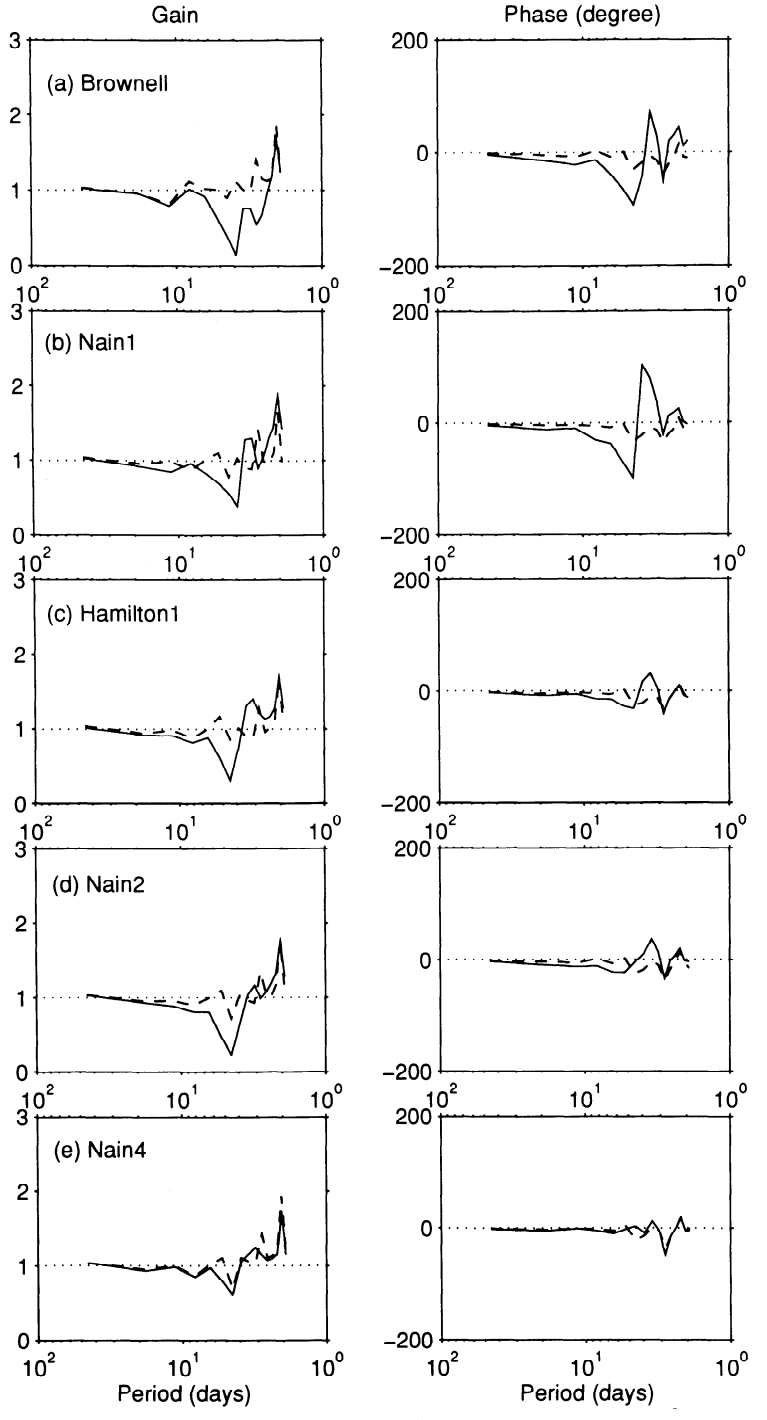

Figure 10. The ratio of the Fourier transform of observed sea level to the inverse barometer for Hudson Bay open (solid line) and closed (dashed line) at (a) Brownell, (b) Nain1, (c) Hamilton1, (d) Nain2, and (e) Nain4.

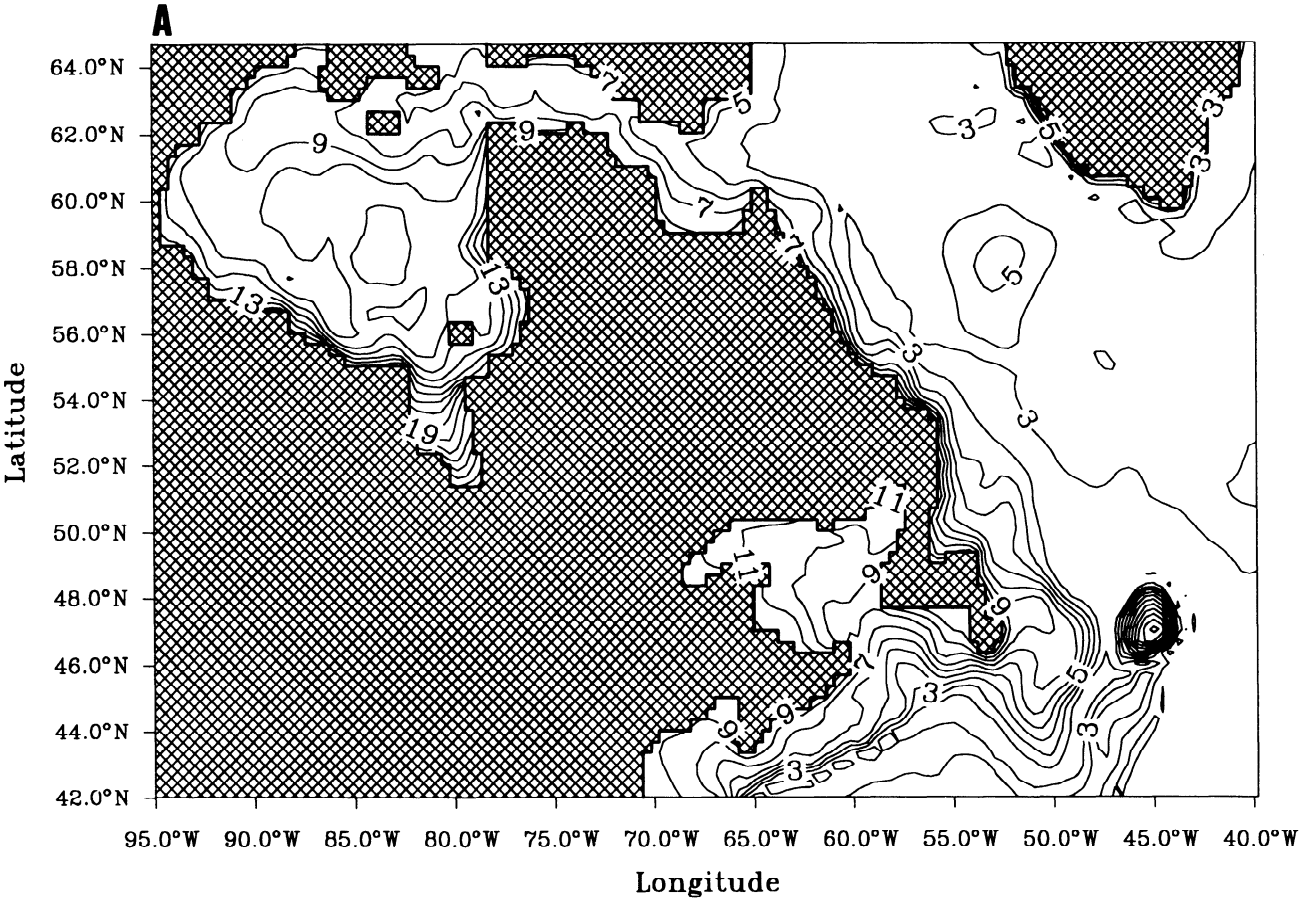

Figure 11. Contours of the root-mean-square sea level response (in centimeters) for (a) the wind- and pressure-forced case, (b) the wind only forced case, and (c) the pressure only forced case. This model run has Hudson Bay open.

quency band over which Hudson Bay influence occurs. The influence of Hudson Bay is clearly greatest near shore and is reduced on the outer shelf (compare Nain4 with Nain1).

The pattern of observed sea level response can best be seen by plotting the spatial patterns of the root-mean-square variability (Figure 11). These plots show that most of the variance is on the shelf, trapped against the coast. There are, however, some exceptions; for example, the well-defined response over the Flemish Cap, a seamount located at about 48°N 45°W. There is also a maximum in the center of the Labrador Sea, a feature that appears to be driven by wind stress forcing since it is absent in the rms plot for the pressure only case (Figure 11c). The comparison between pressure only and the wind only cases indicates that most of the variance is driven by the wind field. Plots for the same model runs with Hudson Bay closed (not shown) are so similar that it is rather difficult to detect any influence of Hudson Bay. Close inspection, however, reveals that there are differences on the inner part of the shelf, close to the coast. The response in the Labrador Sea does not appear to be influenced by the presence of Hudson Bay.

4. Summary and Conclusions

We have shown that a high-resolution, barotropic model of the North Atlantic can successfully simulate most of the observed bottom pressure variability on the Newfoundland and Labrador Shelves. The model is driven by twice-daily, ECMWF analyses of wind and atmospheric pressure. A significant nonisostatic response in the observed data at timescales of 4–10 days is reproduced in the model by including Hudson Bay in the model domain. On the northern end of the Labrador Shelf, pressure and wind forcing are roughly equally important. Farther south, wind forcing dominates. Across the shelf the model shows decreasing coherence with the data.

Coherence at longer periods (10–30 days) is also significant, although the model does not capture the tendency of increasing energy with decreasing frequency seen in the observed data. The success of the barotropic model confirms the relatively unimportant role played by stratification, at least at these time-scales. This is because length scales, e.g., the shelf width, are large compared to the internal radius of deformation [*Middleton and Wright,* 1990].

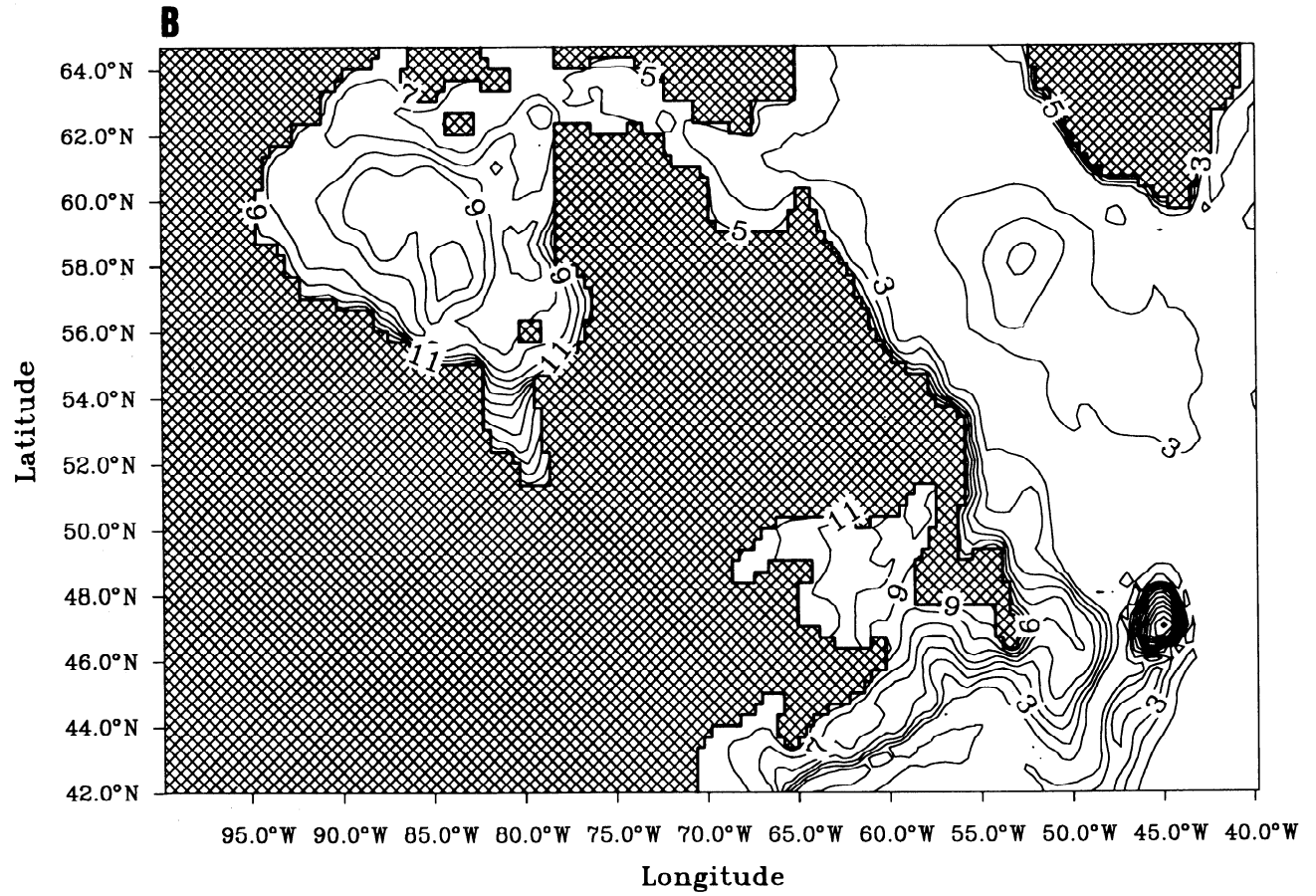

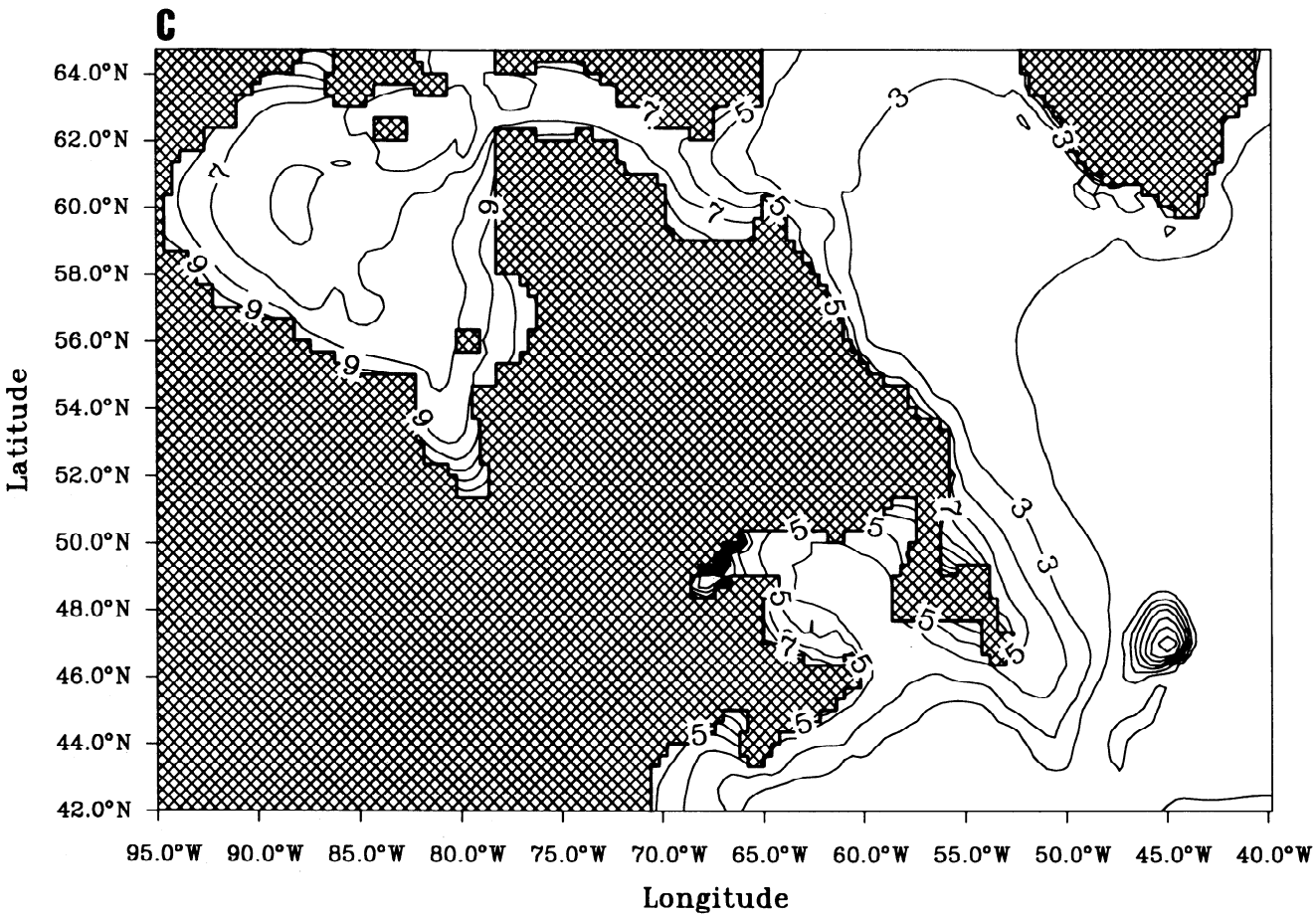

Figure 11. (continued)

The best agreement between the model and the data is obtained at the northern end of the Labrador Shelf and on the Grand Banks. Since coastal trapped waves travel from north to south, we might expect the model to perform better in the north. This is because even at the resolution used in this study, we may not be adequately modeling the scattering of energy by the topography. This could explain the somewhat reduced coherence between model and data as one moves southward along the shelf. To properly account for the along shelf scattering, an even higher-resolution model, including stratification, may be required (as length scales approach the internal radius of deformation scale, typically 5 km, stratification effects will become increasingly necessary to properly model the scattering process). The strong agreement between the model and the data on the Grand Banks can be explained by the presence of closed isobaths, which insulate the banks from remote influences (such as from the Labrador Shelf).

Near the shelf break the model shows relatively poor agreement with observation, consistent with the study of *deYoung et al.* [1992]. Perhaps the reasons for this discrepancy are the imperfect formulation of the bottom and coastal topography and the absence of stratification, although other factors may also be important. The influence of mesoscale eddies has been suggested previously [*LeBlond*, 1982; *Ikeda*, 1987] and might be expected to have an important influence near the shelf break. It may also be that because of the much lower signal-to-noise ratio on the outer shelf (Figure 3), the observations simply do not resolve the shelf wave signal.

Numerical experiments conducted with Hudson Bay open and closed confirm the hypothesis of *Wright et al.* [1987], later extended by *Webster and Narayanan* [1988], that Hudson Bay exerts an influence on the Labrador Shelf. Our results confirm that under atmospheric pressure forcing the bay/strait system generates a significantly nonisostatic response on the Labrador Shelf, at periods of 4-10 days, roughly corresponding to the Helmholtz resonance period (~3.4 days) deduced by *Wright et al.* [1987]. The Hudson Bay open and closed tests also show that both wind and atmospheric pressure forcing over Hudson Bay and Hudson Strait must be included to account for the observed nonisostatic response first reported by *Garrett et al.* [1985].

Acknowledgments. We would like to thank K. Forward, A. Goulding, Y. Ren, and Todd Wareham for their computer assistance. J. Simmons helped in producing the camera-ready copy. We are grateful to D. Wright, who made available the bottom pressure data and also stimulated our initial interest in these problems. Financial support was provided by the Natural Sciences and Engineering Research Council of Canada in the form of research grants to B.deY. and R.J.G. and a collaborative research initiative grant that supports Canadian University activities in the World Ocean Circulation Experiment (WOCE).

References

Akima, H., A method of bivariate interpolation and smooth surface fitting for irregularly distributed data points, *Assoc. Comput. Mach. Trans. Math. Software, 4*(2), 148-159, 1978.

Bryan, F.O., and W.R. Holland, A high resolution simulation of the wind- and thermohaline driven circulation in the North Atlantic Ocean in *Parameterization of Small-Scale Processes, Proceedings of 'Aha Huliko'a Hawaiin Winter Workshop'*, edited by P. Müller and D. Henderson, pp. 99-115, University of Hawaii at Manoa, 1989.

Bryan, K., A numerical method for the study of the circulation of the world ocean, *J. Comput. Phys., 3,* 347-376, 1969.

Davis, R. E., and P. S. Bogden, Variability on the California shelf forced by local and remote winds during the Coastal Ocean Dynamics Experiment, *J. Geophys. Res., 94,* 4763-4784, 1989.

deYoung, B., R. J. Greatbatch, A. D. Goulding, and K. Venguswamy, Bottom pressure variability on the Labrador Shelf: Model-data comparisons, *J. Geophys. Res., 97,* 11,323-11,331, 1992.

Garrett, C., F. Majaess, and B. Toulany, Sea-level response at Nain, Labrador, to atmospheric pressure and wind, *Atmos. Ocean, 23,* 95-117, 1985.

Gill, A. E., *Atmosphere-Ocean Dynamics*, Academic, San Diego, 1982.

Greatbatch, R. J., and A. Goulding, Seasonal variations in a linear barotropic model of the North Atlantic driven by the Hellerman Rosenstein wind stress field, *J. Phys. Oceanogr., 19,* 572-595, 1989.

Greatbatch, R. J., B. deYoung, A. Goulding, and J. Craig, On the influence of local and North Atlantic wind forcing on the seasonal variation of sea level on the Newfoundland and Labrador shelf, *J. Geophys. Res., 95,* 5279-5289, 1990.

Heaps, N. S., On the numerical solution of the three-dimensional hydrodynamical equations for tides and storm surges, *Mem. Soc. R. Sci. Liege, I,* 143-180, 1971.

Hellerman, S., and M. Rosenstein, Normal monthly wind stress over the world ocean with error estimates, *J. Phys. Oceanogr., 13,* 1093-1104, 1983.

Ikeda, M., Modeling interpretation of mesoscale meanders of the ice edge off the Labrador coast observed in NOAA satellite imagery, *J. Phys. Oceanogr., 17,* 1468-1483, 1987.

Large, W. G., and S. Pond, Open ocean momentum flux measurements in moderate strong winds, *J. Phys. Oceanogr., 11,* 324-336, 1981.

LeBlond, P. H., Satellite observations of Labrador Current undulations, *Atmos. Ocean, 20,* 129-142, 1982.

Middleton, J. F., and D. G. Wright, Coastally trapped waves on the Labrador Shelf, Can. Tech. Rep. Hydrogr. Ocean Sci. 116, Dept. of Fish. and Oceans, Ottawa, 1989.

Middleton, J. F., and D. G. Wright, Coastally trapped waves in a stratified ocean, *J. Phys. Oceanogr., 20,* 1521-1527, 1990.

Middleton, J. F., and D. G. Wright, Coastal-trapped waves on the Labrador Shelf, *J. Geophys. Res., 96,* 2599-2617, 1991.

Ponte, R. M., D. A. Salstein, and R. D. Rosen, Sea level response to ressure forcing in a barotropic numerical model, *J. Phys. Oceanogr., 21,* 1043-1057, 1991.

Thompson, K. R., J. R. N. Lazier, and B. Taylor, Wind-forced changes in Labrador Current transport, *J. Geophys. Res., 91,* 14,261-14,268, 1986.

Webster, I., and S. Narayanan, Low-frequency current variability on the Labrador Shelf, *J. Geophys. Res., 93,* 8163-8173, 1988.

Wright, D. G., D. A. Greenberg, and F. G. Majaess, The influence of bays on adjusted sea level over adjacent shelves with application to the Labrador Shelf, *J. Geophys. Res., 92,* 14,610-14,620, 1987.

Wright, D. G., J. R. N. Lazier, and W. Armstrong, Moored

current and pressure data from the Labrador/Newfoundland Shelf, June 1985-July 1987, Can. Tech. Rep. Hydrogr. Ocean Sci. 62, Dept. of Fish. and Oceans, Ottawa, 1988.

Wright, D. G., D. A. Greenberg, and J. F. Middleton, Statistical estimates and dynamical interpretations of bottom pressure variations over the Labrador/Newfoundland Shelf, Can. Tech. Rep. Hydrogr. Ocean Sci. 131, Dept. of Fish. and Oceans, Ottawa, 1991.

Wunsch, C., Bermuda sea level relation to tides, weather and baroclinic fluctuations, *Rev. Geophys., 10*, 1-49, 1972.

Brad deYoung, Youyu Lu, and Richard J. Greatbatch, Department of Physics, Memorial University of Newfoundland, St. John's, Canada A1B 3X7 (email: bdeyoung@crosby.physics.mun.ca)

(Received May 19, 1994; revised December 6, 1994; accepted January 18, 1995.)